Supporting Information

A bimetallic MOF-derived spiral-shaped α-Fe_2O_3/In_2O_3 heterojunction for cyclohexane gas sensor

Dan Xie[a], Feng Zhang*[a,b], Kai Yu[a], Xiaofeng Li*[a] and Fengyu Qu*[a,b]

[a.] *Key Laboratory of Photochemical Biomaterials and Energy Storage Materials, Heilongjiang Province and School of Chemistry and Chemical Engineering, Harbin Normal University, Harbin 150025, P. R. China*

[b.] *Key Laboratory of Photonic and Electronic Bandgap Materials, Ministry of Education, Harbin Normal University, Harbin 150025, P. R. China*

** Corresponding authors: Feng Zhang (E-mail: zhangfeng@hrbnu. edu. cn) Fengyu Qu (E-mail: qufengyu@hrbnu. edu. cn) and Xiaofeng Li (Lixiaofeng@hrbnu.edu.cn.)*

Preparation of pristine α-Fe_2O_3.

The preparation of pristine α-Fe_2O_3 was as follows[1]: $FeCl_3 \cdot 6H_2O$ (0.249 g) and terephthalic acid (0.153 g) were dissolved in 10 mL and 5 mL DMF under vigorous stirring, respectively. Then, the $FeCl_3$ mixed solution was slowly added into terephthalic acid solution. Whereafter, the as-prepared mixed solution was transferred into a 50 mL Teflon-lined stainless-steel autoclave and reacted at 120 °C for 16 h. The precipitate was washed with DMF and alcohol several times. Finally, the products were fully dried with vacuum at 120 °C for 12 h, and then calcined at 500 °C for 2 h.

Preparation of pristine In_2O_3

The preparation of pristine α-Fe_2O_3 was as follows[2]: the $InCl_3$•$4H_2O$ (0.4 mmol) was dissolved in DI water (26 mL) under continuous magnetic stirring for 10 min, and $CO(NH_2)_2$ (2 mmol) was added into the solution above. Next, the solution was under vigorous stirring until a transparent solution was formed. Then, the mixture was transferred to a Teflon-lined stainless steel reactor kettle and heated at 140 °C for 24 h. After finishing the hydrothermal process, the products were centrifuged and washed for purification with DI water and absolute ethanol. The as-obtained yellow samples were dried at 60 °C for overnight. Finally, the products were heated at 500 °C for 2 h with a slow heating rate of 1 °C min^{-1}.

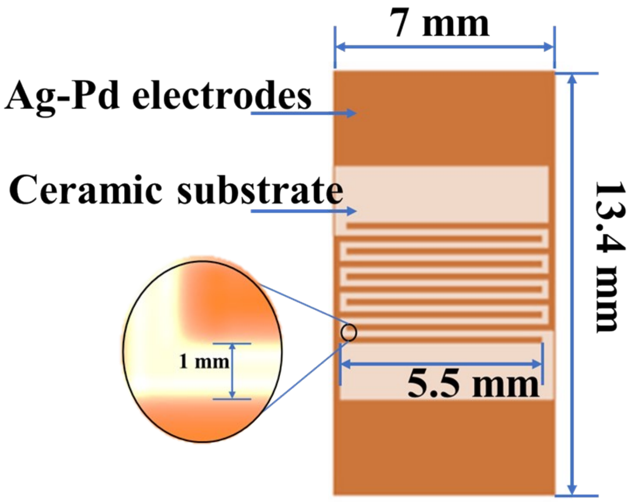

Scheme S1 The schematic of Ag-Pd interdigital electrodes.

The ceramic substrate ($13.4 \times 7\ mm^2$) comprising five parallel Ag-Pd signal electrodes were used while for gas sensing characteristics. The width of each electrode and the distance between two adjacent electrodes was ~ 1.0 mm. The corresponding picture has been shown in the supporting information.

Gas-sensing measurements:

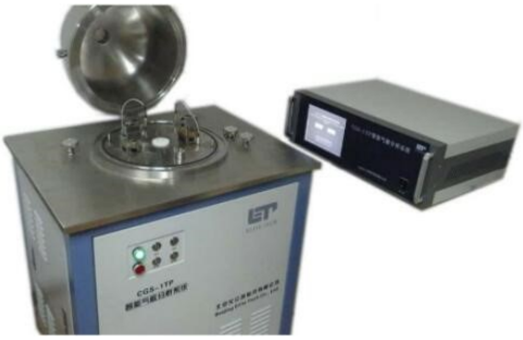

The CGS-1TP directly controls the temperature of the device by external temperature control, so there is no need to make heating wires on the device. The system supports high vacuum pumping, and the measured planar structure sensor substrate can be directly combined with the synthesis process of the material. The CGS-1TP communicates with the computer through the USB interface, collects data in real time and at high speed, and enables direct online analysis of the sensor characteristics. The test process is divided into steps: sample making, connecting samples and test system, setting test conditions, and testing gas sensitivity characteristics (liquid intake mode).

Gas sensing measurement uses a syringe to inject the measured liquid into the test chamber and volatilize it into vapor at high temperature for measurement. The liquid volume corresponding to the different concentrations of the gas is calculated according to the formula.

$$Q = \frac{V \times C \times M}{22.4 \times d \times \rho} \times 10^{-9} \times \frac{273 + T_R}{273 + T_B}$$

where Q is the volume of the liquid, V is the volume of the test chamber, C is the concentration of liquid vapor, M is the molecular weight of the liquid, d is the purity of the liquid, ρ is liquid density, T_R is room temperature and T_B is the temperature in the test chamber.

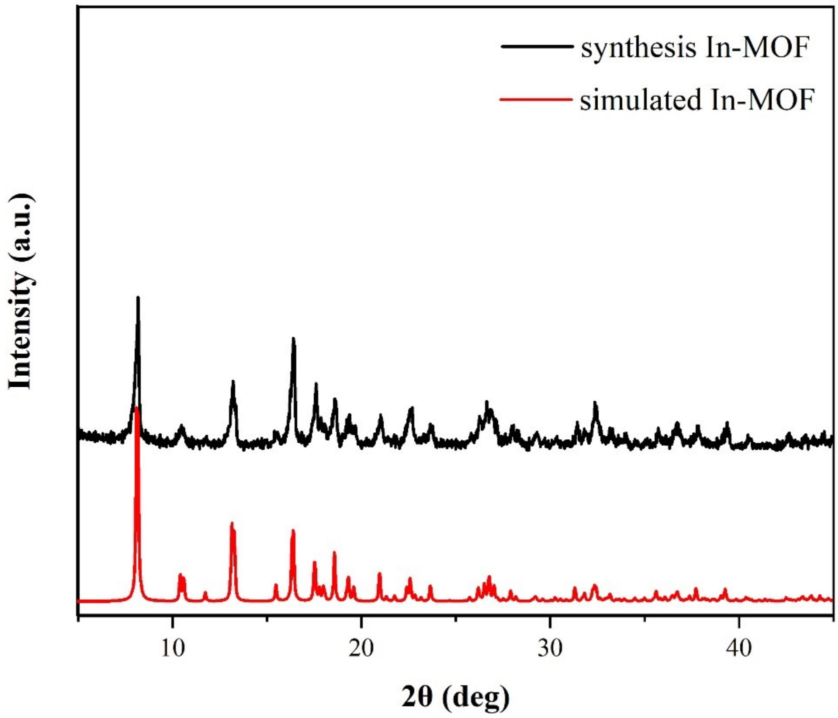

Fig. S1 The XRD pattern of InFc MOF.

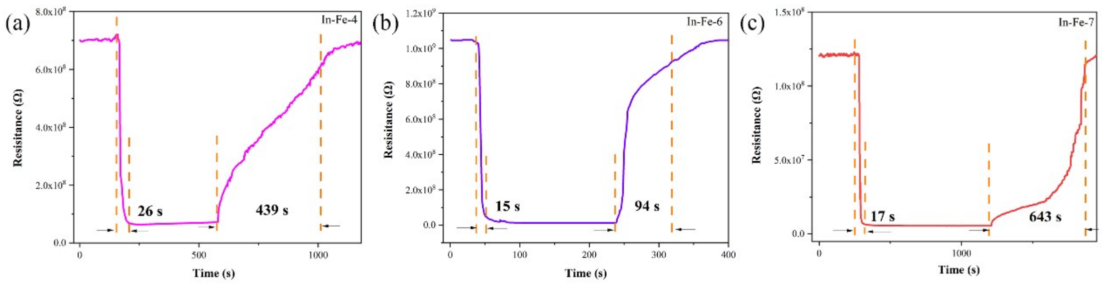

Fig. S2 The response and recovery times of In-Fe-x (x = 4, 6, 7) for cyclohexane sensing.

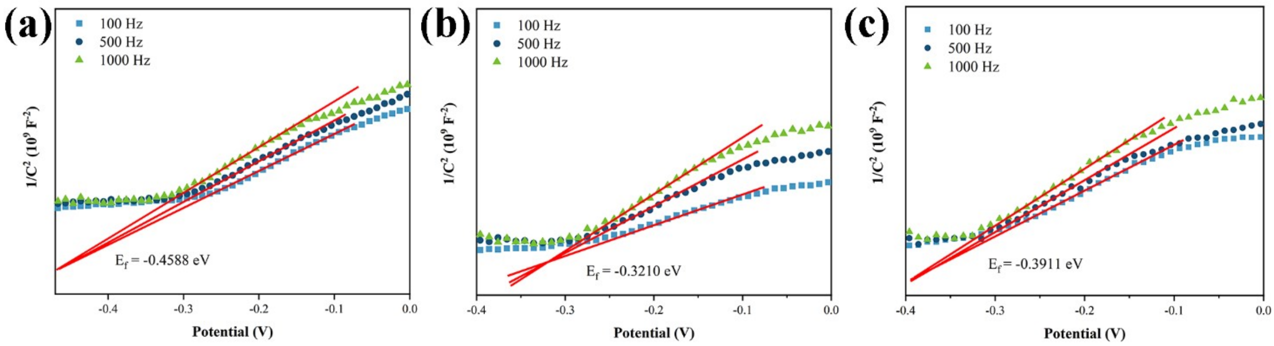

Fig. S3 Mott-Schotty plots of In-Fe-x (x = 4 (a), 6 (b) and 7 (c)) at 100, 500 and 1000 Hz, respectively.

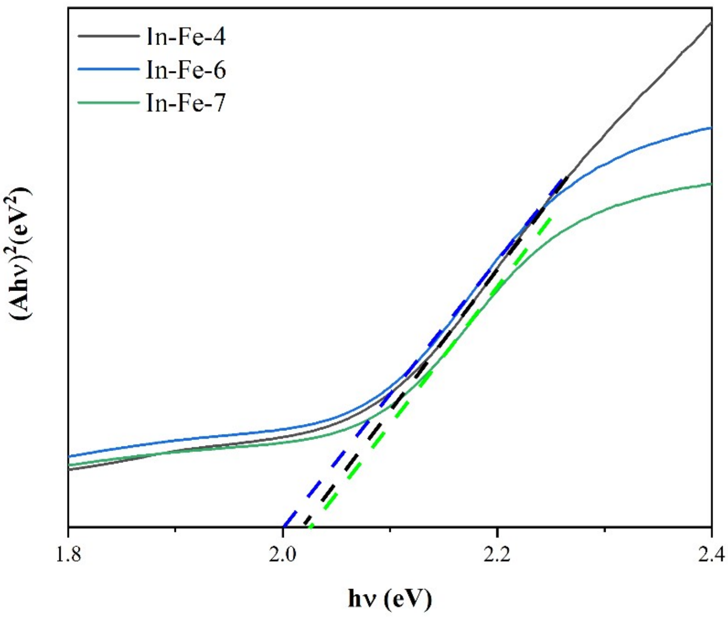

Fig. S4 Tauc plots of In-Fe-x.

Table S1 The average crystallite sizes of In_2O_3 and Fe_2O_3

Sample name	2θ (degree)	(h k l)	Crystallite sizes (nm)
In_2O_3	30.6	(2 2 2)	17
	35.5	(4 0 0)	19
Fe_2O_3	33.2	(1 0 4)	18
	35.6	(1 1 0)	19

Table S2 The S_{BET} and pore size of In-Fe-x.

	S_{BET} (m^2 g^{-1})	Pore size (nm)
In-Fe-4	77.7	2.4
In-Fe-6	50.8	2.4
In-Fe-7	39.2	2.4

Table S3 The list of related parameters from In-Fe-x.

	In-Fe-4	In-Fe-6	In-Fe-7
O_s/O (%)[a]	45	58	46
E_{CB} (eV) vs SCE[b]	-0.4588	-0.3210	-0.3911
E_{VB} (eV) vs SCE[b]	-2.4688	-2.3210	-2.4111
N_D (cm^{-3})[c]	5.8×10^{20}	6.5×10^{20}	6.1×10^{20}
Band-gap width (eV)[d]	2.01	2.00	2.02

a. The molar fraction (%) obtained by XPS spectra.
b. Data obtained by Mott-Schottky and UV-vis spectra.
c. The carrier densities obtained by Mott-Schottky characterization.
d. The band-gap width obtained by UV-vis spectra.

Table S4 The comparison of sensing properties to cyclohexane in this work and reported literatures.

Material	Concentration (ppm)	Sensitivity	Operating temperature (°C)	Ref.
Porous CuO	100	1.1	400	[3]
CuO/ZnO	200	1.3	240	[4]
SnO_2	1	2	280	[5]
WO_3/graphene	100	2.3	275	[6]
Fe_2O_3/ZnO	100	2.89	320	[7]
WO_3 nanotube	100	5	300	[8]
Y_2O_3/In_2O_3	200	57	RT	[9]
In-Fe-6	100	86	225	This work

Reference

1. S. Xiong, X. Lin, S. Liu, S. Weng, S. Jiang, Y. Jiao, Y. Xu and J. Cheng, *Vacuum*, 2020, **182**, 109692.
2. N. Sui, S. Cao, P. Zhang, T. Zhou and T. Zhang, *J. Hazard. Mater.*, 2021, **418**, 126290.
3. G. Zhu, H. Xu, Y. Xiao, Y. Liu, A. Yuan and X. Shen, *ACS Applied Materials & Interfaces*, 2012, **4**, 744-751.
4. C. Yang, X. Cao, S. Wang, L. Zhang, F. Xiao, X. Su and J. Wang, *Ceram. Int.*, 2015, **41**, 1749-1756.
5. K. Kim, P. G. Choi, T. Itoh and Y. Masuda, *ACS Appl Mater Interfaces*, 2020, **12**, 51637-51644.
6. X. An, J. C. Yu, Y. Wang, Y. Hu, X. Yu and G. Zhang, *J. Mater. Chem.*, 2012, **22**.
7. S. Si, C. Li, X. Wang, Q. Peng and Y. Li, *Sensors Actuators B: Chem.*, 2006, **119**, 52-56.
8. J. Li, J. Zhu and X. Liu, *New J. Chem.*, 2013, **37**.
9. J. Shruthi, N. Jayababu, P. Ghosal and M. V. Ramana Reddy, *Ceram. Int.*, 2019, **45**, 21497-21504.